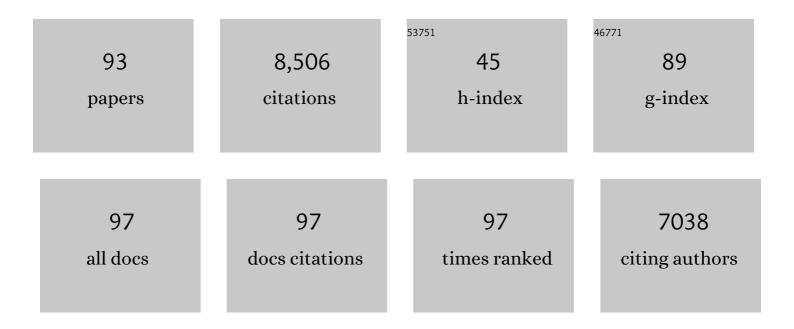
## Penelope King

List of Publications by Year in descending order

Source: https://exaly.com/author-pdf/6398251/publications.pdf Version: 2024-02-01



DENELODE KINC

#	Article	IF	CITATIONS
1	Characterization and Origin of Aluminous A-type Granites from the Lachlan Fold Belt, Southeastern Australia. Journal of Petrology, 1997, 38, 371-391.	1.1	981
2	A Habitable Fluvio-Lacustrine Environment at Yellowknife Bay, Gale Crater, Mars. Science, 2014, 343, 1242777.	6.0	687
3	Mars' Surface Radiation Environment Measured with the Mars Science Laboratory's Curiosity Rover. Science, 2014, 343, 1244797.	6.0	475
4	Volatile, Isotope, and Organic Analysis of Martian Fines with the Mars Curiosity Rover. Science, 2013, 341, 1238937.	6.0	367
5	SIMS analysis of volatiles in silicate glasses. Chemical Geology, 2002, 183, 99-114.	1.4	330
6	Abundance and Isotopic Composition of Gases in the Martian Atmosphere from the Curiosity Rover. Science, 2013, 341, 263-266.	6.0	327
7	Martian Fluvial Conglomerates at Gale Crater. Science, 2013, 340, 1068-1072.	6.0	326
8	Are Aâ€ŧype granites the highâ€ŧemperature felsic granites? Evidence from fractionated granites of the Wangrah Suite. Australian Journal of Earth Sciences, 2001, 48, 501-514.	0.4	324
9	Volatile and Organic Compositions of Sedimentary Rocks in Yellowknife Bay, Gale Crater, Mars. Science, 2014, 343, 1245267.	6.0	323
10	Elemental Geochemistry of Sedimentary Rocks at Yellowknife Bay, Gale Crater, Mars. Science, 2014, 343, 1244734.	6.0	246
11	Soil Diversity and Hydration as Observed by ChemCam at Gale Crater, Mars. Science, 2013, 341, 1238670.	6.0	215
12	Evidence for indigenous nitrogen in sedimentary and aeolian deposits from the <i>Curiosity</i> rover investigations at Gale crater, Mars. Proceedings of the National Academy of Sciences of the United States of America, 2015, 112, 4245-4250.	3.3	172
13	Accommodation of the carbonate ion in apatite: An FTIR and X-ray structure study of crystals synthesized at 2–4 GPa. American Mineralogist, 2004, 89, 1422-1432.	0.9	164
14	Effects of H2O, pH, and oxidation state on the stability of Fe minerals on Mars. Journal of Geophysical Research, 2005, 110, .	3.3	156
15	Sulfur on Mars. Elements, 2010, 6, 107-112.	0.5	148
16	The Petrochemistry of Jake_M: A Martian Mugearite. Science, 2013, 341, 1239463.	6.0	134
17	The origin and implications of clay minerals from Yellowknife Bay, Gale crater, Mars. American Mineralogist, 2015, 100, 824-836.	0.9	122
18	Geochemical diversity in first rocks examined by the Curiosity Rover in Gale Crater: Evidence for and significance of an alkali and volatileâ€rich igneous source. Journal of Geophysical Research E: Planets, 2014, 119, 64-81.	1.5	113

PENELOPE KING

#	Article	IF	CITATIONS
19	Calibration of the Mars Science Laboratory Alpha Particle X-ray Spectrometer. Space Science Reviews, 2012, 170, 319-340.	3.7	105
20	Low Upper Limit to Methane Abundance on Mars. Science, 2013, 342, 355-357.	6.0	103
21	Sulfur degassing at Erta Ale (Ethiopia) and Masaya (Nicaragua) volcanoes: Implications for degassing processes and oxygen fugacities of basaltic systems. Geochemistry, Geophysics, Geosystems, 2013, 14, 4076-4108.	1.0	100
22	Fractionation of metaluminous A-type granites: an experimental study of the Wangrah Suite, Lachlan Fold Belt, Australia. Precambrian Research, 2003, 124, 327-341.	1.2	95
23	Resolution of bridging oxygen signals from O 1s spectra of silicate glasses using XPS: Implications for O and Si speciation. Geochimica Et Cosmochimica Acta, 2007, 71, 4297-4313.	1.6	95
24	A global Mars dust composition refined by the Alphaâ€Particle Xâ€ray Spectrometer in Gale Crater. Geophysical Research Letters, 2016, 43, 67-75.	1.5	95
25	CO2 solubility and speciation in intermediate (andesitic) melts: the role of H2O and composition. Geochimica Et Cosmochimica Acta, 2002, 66, 1627-1640.	1.6	88
26	Trace element geochemistry (Li, Ba, Sr, and Rb) using <i>Curiosity</i> 's ChemCam: Early results for Gale crater from Bradbury Landing Site to Rocknest. Journal of Geophysical Research E: Planets, 2014, 119, 255-285.	1.5	86
27	Analytical techniques for volatiles: A case study using intermediate (andesitic) glasses. American Mineralogist, 2002, 87, 1077-1089.	0.9	83
28	Porphyry copper deposit formation by sub-volcanic sulphur dioxide flux andÂchemisorption. Nature Geoscience, 2015, 8, 210-215.	5.4	83
29	Mineralogy of the Paso Robles soils on Mars. American Mineralogist, 2008, 93, 728-739.	0.9	80
30	Stevensite in the modern thrombolites of Lake Clifton, Western Australia: A missing link in microbialite mineralization?. Geology, 2014, 42, 575-578.	2.0	74
31	High surface porosity as the origin of emissivity features in asteroid spectra. Icarus, 2012, 221, 1162-1172.	1.1	73
32	Deciphering Biosignatures in Planetary Contexts. Astrobiology, 2019, 19, 1075-1102.	1.5	66
33	The composition and evolution of primordial solutions on Mars, with application to other planetary bodies. Geochimica Et Cosmochimica Acta, 2004, 68, 4993-5008.	1.6	65
34	A new approach to determine and quantify structural units in silicate glasses using micro-reflectance Fourier-Transform infrared spectroscopy. American Mineralogist, 2006, 91, 1783-1793.	0.9	62
35	Matrix effects in hydrogen isotope analysis of silicate glasses by SIMS. Chemical Geology, 2006, 235, 352-365.	1.4	61
36	Non-basaltic asteroidal magmatism during the earliest stages of solar system evolution: A view from Antarctic achondrites Graves Nunatak 06128 and 06129. Geochimica Et Cosmochimica Acta, 2010, 74, 1172-1199.	1.6	59

Penelope King

#	Article	IF	CITATIONS
37	SULFUR K-EDGE XANES SPECTROSCOPY: CHEMICAL STATE AND CONTENT OF SULFUR IN SILICATE GLASSES. Canadian Mineralogist, 2005, 43, 1605-1618.	0.3	58
38	Planning for Mars Returned Sample Science: Final Report of the MSR End-to-End International Science Analysis Group (E2E-iSAG). Astrobiology, 2012, 12, 175-230.	1.5	58
39	Volcanic gas composition, metal dispersion and deposition during explosive volcanic eruptions on the Moon. Geochimica Et Cosmochimica Acta, 2017, 206, 296-311.	1.6	57
40	Oxy-substitution and dehydrogenation in mantle-derived amphibole megacrysts. Geochimica Et Cosmochimica Acta, 1999, 63, 3635-3651.	1.6	55
41	Partitioning of Fe3+/Fetotal between amphibole and basanitic melt as a function of oxygen fugacity. Earth and Planetary Science Letters, 2000, 178, 97-112.	1.8	54
42	Volatile-rich silicate melts from Oldoinyo Lengai volcano (Tanzania): Implications for carbonatite genesis and eruptive behavior. Earth and Planetary Science Letters, 2013, 361, 379-390.	1.8	53
43	Correlations of octahedral cations with OH <sup>â^'</sup> , O <sup>2â^'</sup> , Cl <sup>â^'</sup> , and F <sup>â^'</sup> in biotite from volcanic rocks and xenoliths. American Mineralogist, 2002, 87, 142-153.	0.9	51
44	Chemistry and texture of the rocks at Rocknest, Gale Crater: Evidence for sedimentary origin and diagenetic alteration. Journal of Geophysical Research E: Planets, 2014, 119, 2109-2131.	1.5	48
45	Stability of hydrated minerals on Mars. Geophysical Research Letters, 2007, 34, .	1.5	46
46	Fractionation vs. magma mixing in the Wangrah Suite A-type granites, Lachlan Fold Belt, Australia: Experimental constraints. Lithos, 2008, 102, 415-434.	0.6	46
47	Asteroid (21) Lutetia as a remnant of Earth's precursor planetesimals. Icarus, 2011, 216, 650-659.	1.1	45
48	Characteristics of pebble―and cobbleâ€sized clasts along the Curiosity rover traverse from Bradbury Landing to Rocknest. Journal of Geophysical Research E: Planets, 2013, 118, 2361-2380.	1.5	44
49	Gas–Solid Reactions: Theory, Experiments and Case Studies Relevant to Earth and Planetary Processes. Reviews in Mineralogy and Geochemistry, 2018, 84, 1-56.	2.2	39
50	Mineralogical and spectroscopic investigation of the Tagish Lake carbonaceous chondrite by X-ray diffraction and infrared reflectance spectroscopy. Meteoritics and Planetary Science, 2010, 45, 675-698.	0.7	38
51	Gale crater and impact processes – Curiosity's first 364 Sols on Mars. Icarus, 2015, 249, 108-128.	1.1	37
52	Characterization of halophiles in natural MgSO4 salts and laboratory enrichment samples: Astrobiological implications for Mars. Planetary and Space Science, 2010, 58, 599-615.	0.9	34
53	Effect of SiO2, total FeO, Fe3+/Fe2+, and alkali elements in basaltic glasses on mid-infrared spectra. American Mineralogist, 2009, 94, 1580-1590.	0.9	33
54	Elemental Composition and Chemical Evolution of Geologic Materials in Gale Crater, Mars: APXS Results From Bradbury Landing to the Vera Rubin Ridge. Journal of Geophysical Research E: Planets, 2020, 125, e2020JE006536.	1.5	33

PENELOPE KING

#	Article	IF	CITATIONS
55	Mid-infrared emission spectroscopy and visible/near-infrared reflectance spectroscopy of Fe-sulfate minerals. American Mineralogist, 2015, 100, 66-82.	0.9	32
56	Thermal infrared reflectance and emission spectroscopy of quartzofeldspathic glasses. Geophysical Research Letters, 2007, 34, .	1.5	31
57	The Methane Diurnal Variation and Microseepage Flux at Gale Crater, Mars as Constrained by the ExoMars Trace Gas Orbiter and Curiosity Observations. Geophysical Research Letters, 2019, 46, 9430-9438.	1.5	31
58	The oxygen-isotope composition of chondrules and isolated forsterite and olivine grains from the Tagish Lake carbonaceous chondrite. Geochimica Et Cosmochimica Acta, 2010, 74, 2484-2499.	1.6	30
59	SO2 Gas Reactions with Silicate Glasses. Reviews in Mineralogy and Geochemistry, 2018, 84, 229-255.	2.2	28
60	Radiocarbon age constraints for a Pleistocene–Holocene transition rock art style: The Northern Running Figures of the East Alligator River region, western Arnhem Land, Australia. Journal of Archaeological Science: Reports, 2017, 11, 80-89.	0.2	27
61	The Mars Science Laboratory APXS calibration target: Comparison of Martian measurements with the terrestrial calibration. Nuclear Instruments & Methods in Physics Research B, 2014, 323, 49-58.	0.6	26
62	Sulfur on Mars from the Atmosphere to the Core. , 2019, , 119-183.		25
63	Rapid water exsolution, degassing, and bubble collapse observed experimentally in K-phonolite melts. Journal of Volcanology and Geothermal Research, 2008, 173, 178-184.	0.8	24
64	Microbeam X-ray analysis of Ce3+/Ce4+ in Ti-rich minerals: A case study with titanite (sphene) with implications for multivalent trace element substitution in minerals. American Mineralogist, 2013, 98, 110-119.	0.9	23
65	FTIR micro-reflectance measurements of the CO 3 2- ion content in basanite and leucitite glasses. Contributions To Mineralogy and Petrology, 1996, 125, 311-318.	1.2	22
66	Development of a new laboratory technique for highâ€ŧemperature thermal emission spectroscopy of silicate melts. Journal of Geophysical Research: Solid Earth, 2013, 118, 1968-1983.	1.4	22
67	Mineralogical and spectroscopic investigation of enstatite chondrites by Xâ€ray diffraction and infrared reflectance spectroscopy. Journal of Geophysical Research, 2010, 115, .	3.3	20
68	Methods to analyze metastable and microparticulate hydrated and hydrous iron sulfate minerals. American Mineralogist, 2011, 96, 1856-1869.	0.9	20
69	A micro-reflectance IR spectroscopy method for analyzing volatile species in basaltic, andesitic, phonolitic, and rhyolitic glasses. American Mineralogist, 2013, 98, 1162-1171.	0.9	20
70	Unravelling the Consequences of SO2–Basalt Reactions for Geochemical Fractionation and Mineral Formation. Reviews in Mineralogy and Geochemistry, 2018, 84, 257-283.	2.2	18
71	Refinement of the Compton–Rayleigh scatter ratio method for use on the Mars Science Laboratory alpha particle X-ray spectrometer. Nuclear Instruments & Methods in Physics Research B, 2013, 302, 24-31.	0.6	17
72	High temperature gas–solid reactions in calc–silicate Cu–Au skarn formation; Ertsberg, Papua Province, Indonesia. Contributions To Mineralogy and Petrology, 2017, 172, 1.	1.2	17

PENELOPE KING

#	Article	lF	CITATIONS
73	Accurate predictions of microscale oxygen barometry in basaltic glasses using V K-edge X-ray absorption spectroscopy: A multivariate approach. American Mineralogist, 2018, 103, 1282-1297.	0.9	16
74	MSL-APXS titanium observation tray measurements: Laboratory experiments and results for the Rocknest fines at the <i>Curiosity</i> field site in Gale Crater, Mars. Journal of Geophysical Research E: Planets, 2014, 119, 1046-1060.	1.5	13
75	Analytical Techniques for Probing Small-Scale Layers that Preserve Information on Gas–Solid Interactions. Reviews in Mineralogy and Geochemistry, 2018, 84, 103-175.	2.2	13
76	Vaporâ€deposited minerals contributed to the martian surface during magmatic degassing. Journal of Geophysical Research E: Planets, 2019, 124, 1592.	1.5	13
77	Dehydrogenation of kaersutitic amphibole under electron beam excitation recorded by changes in Fe3+/ÂFe: An EMP and SIMS study. American Mineralogist, 2008, 93, 1273-1281.	0.9	12
78	Spectral analysis of synthetic quartzofeldspathic glasses using laboratory thermal infrared spectroscopy. Journal of Geophysical Research, 2010, 115, .	3.3	12
79	Effect of halite coatings on thermal infrared spectra. Journal of Geophysical Research: Solid Earth, 2015, 120, 2162-2178.	1.4	12
80	Ultrashort pulsed laser ablation of granite for stone conservation. Optics and Laser Technology, 2022, 151, 108057.	2.2	12
81	Using Infrared and Raman Spectroscopy to Analyze Gas–Solid Reactions. Reviews in Mineralogy and Geochemistry, 2018, 84, 177-228.	2.2	8
82	Implications of Reactions Between SO <sub>2</sub> and Basaltic Glasses for the Mineralogy of Planetary Crusts. Journal of Geophysical Research E: Planets, 2019, 124, 2563-2582.	1.5	8
83	High resolution 3D mapping of grain kinematics during high temperature sequestration of SO2 from flue gas by carbonate aggregates. Scientific Reports, 2020, 10, 2201.	1.6	8
84	Refinement of the Compton–Rayleigh scatter ratio method for use on the Mars Science Laboratory alpha particle X-ray spectrometer: II – Extraction of invisible element content. Nuclear Instruments & Methods in Physics Research B, 2016, 368, 129-137.	0.6	7
85	An experimental study of SO2 reactions with silicate glasses and supercooled melts in the system anorthite–diopside–albite at high temperature. Contributions To Mineralogy and Petrology, 2019, 174, 1.	1.2	7
86	Prograde and retrograde metasomatic reactions in mineralised magnesium-silicate skarn in the Cu-Au Ertsberg East Skarn System, Ertsberg, Papua Province, Indonesia. Ore Geology Reviews, 2020, 125, 103697.	1.1	6
87	Characterization of mineral coatings associated with a Pleistoceneâ€Holocene rock art style: The Northern Running Figures of the East Alligator River region, western Arnhem Land, Australia. Data in Brief, 2017, 10, 537-543.	0.5	4
88	Prediction of the thermodynamic functions of mixing of binary oxide melts in the PbO–SiO2, Al2O3–SiO2 and CaO–Al2O3 systems by structure-based modification of the quasi-chemical model. Calphad: Computer Coupling of Phase Diagrams and Thermochemistry, 2015, 49, 19-34.	0.7	3
89	3D microstructure controls on mineral carbonation. Journal of CO2 Utilization, 2021, 47, 101494.	3.3	3
90	4. Analytical Techniques for Probing Small-Scale Layers that Preserve Information on Gas–Solid		0

<sup>4.</sup> Analytical Techniques for Probing Interactions. , 2018, , 103-176.

#	Article	IF	CITATIONS
91	1. Gas–Solid Reactions: Theory, Experiments and Case Studies Relevant to Earth and Planetary Processes. , 2018, , 1-56.		0
92	6. SO <sub>2</sub> Gas Reactions with Silicate Glasses. , 2018, , 229-256.		0
93	7. Unravelling the Consequences of SO <sub>2</sub> –Basalt Reactions for Geochemical Fractionation and Mineral Formation. , 2018, , 257-284.		0